

Properties of highly (100) oriented Pb (Mg $1/3$, Nb $2/3$) O 3 – Pb Ti O 3 films on La Ni O 3 bottom electrodes

Y. W. Li, Z. G. Hu, F. Y. Yue, G. Y. Yang, W. Z. Shi, X. J. Meng, J. L. Sun, and J. H. Chu

Citation: [Applied Physics Letters](#) **91**, 232912 (2007); doi: 10.1063/1.2822421

View online: <http://dx.doi.org/10.1063/1.2822421>

View Table of Contents: <http://scitation.aip.org/content/aip/journal/apl/91/23?ver=pdfcov>

Published by the [AIP Publishing](#)

Articles you may be interested in

Enhanced ferroelectric and dielectric properties of highly (100)-oriented 0.67 Pb (Mg $1/3$ Nb $2/3$) O 3 – 0.33 PbTiO 3 thin films with a special Pb (Zr 0.2 , Ti 0.8) O 3 / PbO x bilayered buffer layer

J. Appl. Phys. **104**, 086104 (2008); 10.1063/1.3006139

Electrical and optical properties of Pb (Mg $1/3$ Nb $2/3$) O 3 – PbTiO 3 thin films prepared by chemical solution deposition

Appl. Phys. Lett. **87**, 072903 (2005); 10.1063/1.1999859

Dielectric and electromechanical properties of ferroelectric-relaxor 0.9 Pb(Mg $1/3$ Nb $2/3$) O 3 – 0.1PbTiO 3 thin films

J. Appl. Phys. **90**, 4682 (2001); 10.1063/1.1409573

Dielectric and piezoelectric properties of (x) Pb(Mg $1/3$ Nb $2/3$) O 3 – (1-x) Pb(Zr $1/2$ Ti $1/2$) O 3 thin films prepared by the sol-gel method

J. Appl. Phys. **90**, 1968 (2001); 10.1063/1.1388572

Structural and electrical characteristics of Pb 0.90 La 0.15 TiO 3 thin films on different bottom electrodes

J. Appl. Phys. **89**, 5637 (2001); 10.1063/1.1365062



Properties of highly (100) oriented $\text{Pb}(\text{Mg}_{1/3}, \text{Nb}_{2/3})\text{O}_3\text{-PbTiO}_3$ films on LaNiO_3 bottom electrodes

Y. W. Li,^{a)} Z. G. Hu, and F. Y. Yue

ECNU-SITP Joint Laboratory for Image Information and Department of Electronic Engineering, East China Normal University, Shanghai 200241, People's Republic of China

G. Y. Yang and W. Z. Shi

Department of Physics, East China Normal University, Shanghai 200062, People's Republic of China

X. J. Meng and J. L. Sun

National Laboratory for Infrared Physics, Shanghai Institute of Technical Physics, Chinese Academy of Sciences, Shanghai 200083, People's Republic of China

J. H. Chu

National Laboratory for Infrared Physics, Shanghai Institute of Technical Physics, Chinese Academy of Sciences, Shanghai 200083, People's Republic of China and ECNU-SITP Joint Laboratory for Image Information and Department of Electronic Engineering, East China Normal University, Shanghai 200241, People's Republic of China

(Received 24 October 2007; accepted 15 November 2007; published online 7 December 2007)

The 70% $\text{Pb}(\text{Mg}_{1/3}, \text{Nb}_{2/3})\text{O}_3\text{-30% PbTiO}_3$ (PMNT) films have been fabricated on LaNiO_3 (LNO) coated silicon substrate. The conductive LNO films act as a seed layer for the growth of PMNT films, which depresses the formation of pyrochlore phase and induces the high (100) preferred orientation of perovskite PMNT films. Compared with the PMNT films grown on platinum bottom electrode, the ferroelectric properties of PMNT films grown on LNO are enhanced. The frequency dependence of complex permittivity from PMNT films on LNO is the conjunct result of polarization relaxation and movement of oxygen vacancy, which can be fitted by the function containing Debye and universal dielectric response models, respectively. © 2007 American Institute of Physics. [DOI: 10.1063/1.2822421]

Recently, relaxor ferroelectrics attract many attentions due to their unique ferroelectric and dielectric properties.¹⁻⁵ Because of the large electromechanical coupling factor, large electro-optic coefficient, and excellent piezoelectric properties, $\text{Pb}(\text{Mg}_{1/3}, \text{Nb}_{2/3})\text{O}_3\text{-PbTiO}_3$ (PMNT) is one of the most promising candidates in the family of relaxor ferroelectrics for a variety of integrated device application, such as dynamic random access memories, piezoelectric, and electro-optic devices.⁶⁻⁹ Studies on optical, dielectric, and piezoelectric properties about PMNT single crystal and ceramic have been carried out.¹⁰⁻¹² Compared with single crystal and ceramic, film can be convenient to integrate into devices. PMNT films can be fabricated on single crystal substrates or different electrodes by various methods, such as metal-organic chemical vapor deposition, pulsed laser deposition (PLD), radio frequency sputtering, and sol-gel.¹³⁻¹⁷ The existence of pyrochlore phase depresses the dielectric and ferroelectric performances of PMNT films grown on metal electrodes.^{15,16} It was found that the pyrochlore component in PMNT films can be suppressed by buffer layer between PMNT film and metal electrodes, such as LaNiO_3 (LNO) and $(\text{La}, \text{Sr})\text{CoO}_3$.^{3,18}

As a typical conductive oxide, LaNiO_3 has been used as electrode for ferroelectric films such as $\text{Pb}(\text{Zr}, \text{Ti})\text{O}_3$ and $(\text{Ba}, \text{Sr})\text{TiO}_3$.^{19,20} It was proved that the performance of ferroelectric films can be improved using LNO instead of metal as electrode. It is easy to fabricate LNO on silicon

substrate, by contrast, one or two layers of adhere layer are necessary for metal electrode such as platinum (Pt). Therefore, the structure of ferroelectric/LNO/Si should be simpler than that of ferroelectric/buffer layer/Pt/Ti/SiO₂/Si, which is convenient and useful for the integration of devices. In this letter, we fabricated the PMNT films by PLD method on LNO coated silicon and studied the structural, dielectric, and ferroelectric properties of the PMNT films.

The LNO electrodes were prepared on (100) silicon substrate by chemical solution deposition (CSD).¹⁹ The PMNT films with composition of 70% $\text{Pb}(\text{Mg}_{1/3}, \text{Nb}_{2/3})\text{O}_3\text{-30% PbTiO}_3$ were deposited on LNO coated Si(100) substrate by PLD at the substrate temperature of 650 °C. A KrF excimer laser was used for the deposition with pulse frequency of 5 Hz. The thickness of PMNT films is about 600 nm from profile meter. X-ray diffraction (XRD) was used to analyze the structure and phase composition of the films (D/MAX-2550V, Rigaku Co.). Pt top electrodes with 0.2 mm in diameter were sputtered for electrical measurements. The ferroelectric and dielectric properties of the PMNT films were measured by a ferroelectric test system (Precision LC, Radiant Technologies, Inc.) and a Hewlett-Packard impedance analyzer (model 4194A) in the frequency range of 100 Hz–1 MHz. All of the measurements were carried out at room temperature.

Figure 1 presents the XRD pattern of the PMNT films grown on LNO coated silicon substrate. Compared with the PMNT on Pt reported by previous literatures,^{15,16} the pyrochlore phase is remarkably suppressed. The PMNT films on LNO electrode exhibit (100) preferred orientation. The lattice constants of PMNT and LNO are estimated to be 4.07

^{a)} Author to whom correspondence should be addressed. Electronic mail: ywli@ee.ecnu.edu.cn.

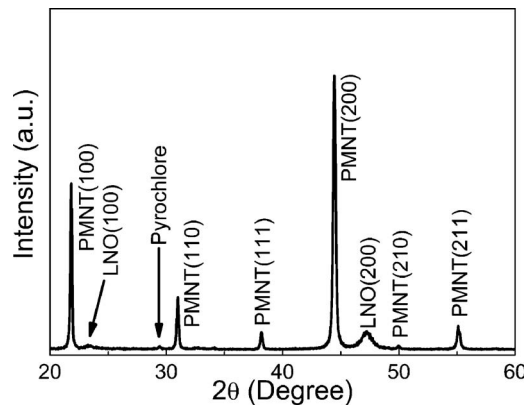


FIG. 1. XRD patterns of PMNT film grown on LNO coated silicon substrate.

and 3.84 Å, respectively. The full width at half maximum of PMNT is greatly smaller than that of LNO, which indicates that the grain size of PMNT prepared by PLD is much larger than that of LNO prepared by CSD.

The hysteretic loop of PMNT on LNO is shown in Fig. 2. The remnant polarization (P_r) and coercive voltage (V_c) are 17.1 $\mu\text{C}/\text{cm}^2$ and 4.09 V at 14 V applied voltage, respectively. It is evident that the ferroelectric properties of PMNT films on LNO are enhanced compared with that of the PMNT films on Pt.¹⁵ The inset of Fig. 2 presents the varieties of P_r and V_c when the applied voltage increases from 4 to 14 V. The increment of coercive voltage becomes gradually flat with applied voltage beyond 10 V, indicating that V_c approaches saturation.

The frequency dependence of complex permittivity (ϵ^*) is shown in Fig. 3. The patterns can be divided into two regions. In the frequency region between 100 Hz and 10 kHz, the real part of complex permittivity (ϵ') decreases slightly with frequency increasing and the imaginary part of complex permittivity (ϵ'') varies moderately. In the frequency region beyond 10 kHz, ϵ' decreases abruptly and a peak of ϵ'' appears. The behavior of complex permittivity in the high frequency region is similar to the relaxation process of polarization, which can be described by modified Debye model,²¹

$$\epsilon^* = \epsilon_\infty + \frac{\epsilon_s - \epsilon_\infty}{1 + (i\omega\tau)^\alpha}, \quad (1)$$

where ϵ_s and ϵ_∞ are static and high frequency dielectric constants, respectively. Here, $\omega = 2\pi f$ is the circle frequency and

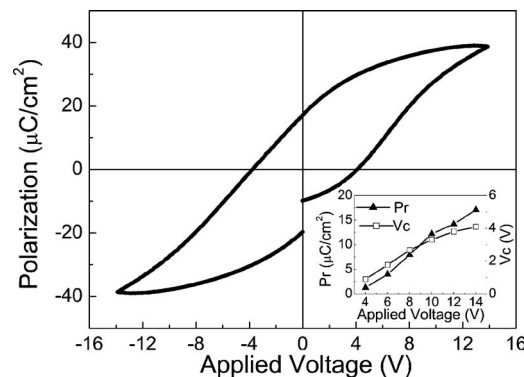


FIG. 2. Hysteretic loop of PMNT film on LNO. The inset shows variety of remnant polarization and coercive voltage with applied voltage.

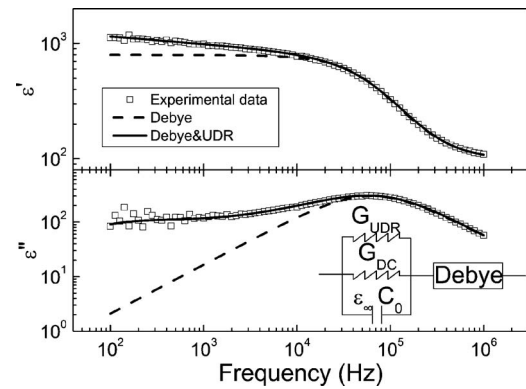


FIG. 3. The frequency dependence of complex permittivity of PMNT film. The inset indicates the equivalent circuit model to delineate the dielectric response of PMNT film.

τ is relaxation time. The parameter α , which is between 0 and 1, is used to index the distribution of relaxation time.²¹ If $\alpha=1$, Eq. (1) gives the result of original Debye model. The fitting results by Eq. (1) are shown in Fig. 3 (dash lines). It is noted that the experimental data at high frequency region can be fitted well, but the deviations between experimental data and model data appear at the low frequency region. Especially, the experimental ϵ'' in the frequency of 100 Hz–1 kHz is one or two magnitude larger than the result of Debye model.

Debye model is used to describe the dielectric performance induced by polar relaxation with single relaxation time. The distribution of relaxation time is taken into account for Cole and Cole's modification.²¹ However, the dielectric contributions by other electric processes (for example, the conductance) are not considered. It is well known that the imaginary part of complex permittivity is related with the real part of complex conductivity (σ^*) by²²

$$\epsilon^*(\omega) = \epsilon'(\omega) - i\epsilon''(\omega) = i\sigma^*(\omega)/\omega\epsilon_0, \quad (2)$$

where ϵ_0 is the vacuum permittivity. Higher ϵ'' at low frequency region means higher conductivity. Therefore, the model described the dielectric response of PMNT on LNO is modified. As shown in the inset of Fig. 3, the equivalent circuit consists of two parts connected in series. One part abides by the Debye model and the contribution of conductance is taken into account in another part.^{22,23} The second part is given by the sum of dc conductivity, the frequency-dependent ac conductivity, and the high frequency dielectric constant ϵ_∞ . The frequency-dependent ac conductivity is depicted by the universal dielectric response (UDR).²² Consequently, the complex conductivity of the second part is given by^{22–25}

$$\sigma_{\text{cond}}^* = \sigma_l' + i\sigma_l'', \quad (3)$$

$$\sigma_l' = \sigma_{\text{dc}} + \sigma_0\omega^s, \quad (4)$$

$$\sigma_l'' = \epsilon_0\epsilon_\infty\omega + \sigma_0 \tan[(\pi/2)s]\omega^s, \quad (5)$$

where σ_{dc} is the dc conductivity and s is a parameter with a value between 0 and 1. From σ_{cond}^* , the complex dielectric permittivity of the second part can be estimated by Eq. (2) and the total complex dielectric permittivity can be calculated. The calculated data is also shown in Fig. 3 (solid line). It is evident that the experimental data can be fitted well in

the two frequency regions. It means that there are some kinds of conductance processes, which have remarkable effects on the dielectric performance of the PMNT films.

It is worthy to discuss the origin of the conductivity for the PMNT films. As we know, UDR is a model to describe the hopping conductivity of localized charge carriers.²² In ferroelectrics, oxygen vacancies act as charged carriers generally. Oxygen vacancies are localized in the corners of octahedral cage of oxygen in perovskite structure ferroelectrics. Under the given applied electric field, they can hop among different oxygen lattice positions. Kobor *et al.* investigated the ac impedance spectroscopy of undoped and manganese doped $\text{Pb}(\text{Zn}_{1/3}\text{Nb}_{2/3})\text{O}_3\text{-PbTiO}_3$ (PZNT) single crystals.²⁶ They found that the conduction behavior induced by oxygen vacancies in PZNT can be modeled by UDR. Therefore, the origin of conductivity for the PMNT films can be ascribed to the movement of oxygen vacancies. The dielectric response of PMNT films on LNO is considered as the combined effects of polar relaxation and oxygen vacancy movement.

In conclusion, the PMNT films grown on LNO coated silicon substrate exhibit (100) preferred orientation. The frequency dependence of complex permittivity can be fitted by the function containing Debye and UDR models.

This work was sponsored by Major State Basic Research Development Program of China (2007CB924900), National Natural Science Foundation of China (No. 60677022), Shanghai Pujiang Program (07PJ14034), Shanghai Municipal Commission of Science and Technology Project (07JC14018), and Shanghai Leading Academic Discipline Project (B411).

¹V. Bobnar, Z. Kutnjak, R. Blinc, and A. Levstik, *Phys. Rev. Lett.* **84**, 5892 (2000).

²T. Y. Koo, P. M. Gehring, G. Shirane, V. Kiryukhin, S.-G. Lee, and S.-W. Cheong, *Phys. Rev. B* **65**, 144113 (2002).

- ³A. Y. Liu, X. J. Meng, J. Q. Xue, J. L. Sun, J. Chen, and J. H. Chu, *Appl. Phys. Lett.* **87**, 072903 (2005).
- ⁴X. Y. Zhao, B. J. Fang, H. Cao, Y. P. Guo, and H. S. Luo, *Mater. Sci. Eng., B* **96**, 254 (2002).
- ⁵J.-H. Park, J. Park, J.-G. Park, B.-K. Kim, and Y. Kim, *J. Eur. Ceram. Soc.* **21**, 1383 (2001).
- ⁶M. Algueró, J. Ricote, R. Jiménez, P. Ramos, J. Carreard, B. Dkhil, J. M. Kiat, J. Holc, and M. Kosec, *Appl. Phys. Lett.* **91**, 112905 (2007).
- ⁷Y. L. Lu, J. J. Zheng, M. C. Golomb, F. L. Wang, H. Jiang, and J. Zhao, *Appl. Phys. Lett.* **74**, 3764 (1999).
- ⁸W. S. Tsang, K. Y. Chan, C. L. Mark, and K. H. Wong, *Appl. Phys. Lett.* **83**, 1599 (2003).
- ⁹S. H. Seo, H. C. Kang, and D. Y. Noh, *Appl. Phys. Lett.* **84**, 3133 (2004).
- ¹⁰X. Wan, H. Xu, T. He, D. Lin, and H. Luo, *J. Appl. Phys.* **93**, 4766 (2003).
- ¹¹J. Peng, H.-S. Luo, D. Lin, H.-Q. Xu, T.-H. He, and W.-Q. Jin, *Appl. Phys. Lett.* **85**, 6221 (2004).
- ¹²Z.-Y. Cheng, R. S. Katiyar, X. Yao, and A. Guo, *Phys. Rev. B* **55**, 8165 (1997).
- ¹³G. R. Bai, S. K. Streiffer, P. K. Baumann, O. Auciello, and K. Ghosh, *Appl. Phys. Lett.* **76**, 3106 (2000).
- ¹⁴N. J. Donnelly, G. Gatalan, C. Morros, R. M. Bowman, and J. M. Gregg, *J. Appl. Phys.* **93**, 9924 (2003).
- ¹⁵A. Laha, S. Bhattacharyya, and S. B. Krupanidhi, *Mater. Sci. Eng., B* **106**, 111 (2004).
- ¹⁶S. Jaydeep, S. Yadav, B. P. Malla, A. R. Kulkarni, and N. Venkatramani, *Appl. Phys. Lett.* **81**, 3840 (2002).
- ¹⁷K. H. Yoon, B. D. Lee, J. Park, and J. H. Park, *J. Appl. Phys.* **90**, 1968 (2001).
- ¹⁸A. Laha, S. Saha, and S. B. Krupanidhi, *Thin Solid Films* **424**, 274 (2003).
- ¹⁹X.-J. Meng, J.-L. Sun, J. Yu, H.-J. Ye, S.-L. Guo, and J.-h. Chu, *Appl. Surf. Sci.* **171**, 68 (2001).
- ²⁰G. S. Wang, J. G. Cheng, X. J. Meng, J. Yu, Z. Q. Lai, J. Tang, S. L. Guo, and J. H. Chu, *Appl. Phys. Lett.* **78**, 4172 (2001).
- ²¹K. S. Cole and R. H. Cole, *J. Chem. Phys.* **9**, 341 (1941).
- ²²P. Lunkenheimer, V. Bobnar, A. V. Pronin, A. I. Ritus, A. A. Volkov, and A. Loidl, *Phys. Rev. B* **66**, 052105 (2002).
- ²³A. Tselev, C. M. Brooks, S. M. Anlage, H. Zheng, L. Salamanca-Riba, R. Ramesh, and M. A. Subramania, *Phys. Rev. B* **70**, 144101 (2004).
- ²⁴A. K. Jonscher, *J. Phys. D* **32**, R57 (1999).
- ²⁵A. K. Jonscher, *Nature (London)* **267**, 673 (1977).
- ²⁶D. Kobor, B. Guiffard, L. Lebrun, A. Hajjaji, and D. Guyomar, *J. Phys. D* **40**, 2920 (2007).